Title

Role of the Srs2-Rad51 Interaction Domain in Crossover Control in *Saccharomyces cerevisiae*.

Journal

Genetics, 212(4)

ISSN

0016-6731

Authors

Jenkins, Shirin S

Gore, Steven

Guo, Xiaoge

et al.

Publication Date

2019-08-01

DOI

10.1534/genetics.119.302337

Peer reviewed

Role of the Srs2–Rad51 Interaction Domain in Crossover Control in *Saccharomyces cerevisiae*

Shirin S. Jenkins,*,[1] Steven Gore,* Xiaoge Guo,†,[2] Jie Liu,* Christopher Ede,*,[3] Xavier Veaute,‡ Sue Jinks-Robertson,† Stephen C. Kowalczykowski,*,§ and Wolf-Dietrich Heyer*,§,[4]

*Department of Microbiology and Molecular Genetics and §Department of Molecular and Cellular Biology, University of California, Davis, California 95616, †Department of Molecular Genetics and Microbiology, Duke University, Durham, North Carolina 27710, and ‡CEA, CIGEx, F-92265 Fontenay-aux-Roses Cedex, France

ORCID ID: 0000-0002-7774-1953 (W.-D.H.)

ABSTRACT *Saccharomyces cerevisiae* Srs2, in addition to its well-documented antirecombination activity, has been proposed to play a role in promoting synthesis-dependent strand annealing (SDSA). Here we report the identification and characterization of an *SRS2* mutant with a single amino acid substitution (*srs2-F891A*) that specifically affects the Srs2 pro-SDSA function. This residue is located within the Srs2–Rad51 interaction domain and embedded within a protein sequence resembling a BRC repeat motif. The *srs2-F891A* mutation leads to a complete loss of interaction with Rad51 as measured through yeast two-hybrid analysis and a partial loss of interaction as determined through protein pull-down assays with purified Srs2, Srs2-F891A, and Rad51 proteins. Even though previous work has shown that internal deletions of the Srs2–Rad51 interaction domain block Srs2 antirecombination activity *in vitro*, the Srs2-F891A mutant protein, despite its weakened interaction with Rad51, exhibits no measurable defect in antirecombination activity *in vitro* or *in vivo*. Surprisingly, *srs2-F891A* shows a robust shift from noncrossover to crossover repair products in a plasmid-based gap repair assay, but not in an ectopic physical recombination assay. Our findings suggest that the Srs2 C-terminal Rad51 interaction domain is more complex than previously thought, containing multiple interaction sites with unique effects on Srs2 activity.

KEYWORDS crossover control; protein interaction; helicase; recombination; DNA repair; genome stability

CELLS possess multiple pathways to respond to the varied types of DNA damage that are caused by both endogenous and exogenous sources. Homologous recombination (HR) is a DNA damage repair/tolerance pathway with the potential to target a variety of DNA lesions, including single-stranded DNA (ssDNA) gaps and double-stranded DNA breaks (DSBs) (Kowalczykowski *et al.* 2016). HR requires the presence of intact homologous DNA donor sequences that serve as templates for the repair or bypass of DNA lesions. For DSBs to be channeled to HR, the broken ends must initially be resected to generate long stretches of 3′ overhang ssDNA (Symington and Gautier 2011). The resulting ssDNA is subsequently coated with Rad51 protomers forming a nucleoprotein filament that carries out two key HR reactions: homology search and DNA strand invasion (Sung 1994). The invading ssDNA 3′ end primes DNA synthesis using the invaded duplex DNA as a repair template (McVey *et al.* 2016). The resulting extended displacement loop structure (D-loop) may then be channeled to one of two main subpathways: synthesis-dependent strand annealing (SDSA) or the double Holliday junction (dHJ) pathway (Jenkins *et al.* 2016). While SDSA produces exclusively noncrossover (NCO) repair products, the dHJ pathway has the potential to produce either crossover (CO) or NCO products depending on how the dHJ intermediate is processed.

Misregulation of HR can lead to genomic rearrangements and overall genomic instability despite its important role in DNA repair. To maintain genome stability, the HR pathway is tightly controlled and regulated at multiple steps. Since Rad51 filament formation is a crucial step in initiating the

doi: https://doi.org/10.1534/genetics.119.302337
Manuscript received May 15, 2019; accepted for publication May 22, 2019; published Early Online May 29, 2019
Available freely online through the author-supported open access option.
Supplemental material available at FigShare: https://doi.org/10.25386/genetics.8179493.
[1]Present address: Department of Molecular and Cell Biology, University of California, Berkeley, Berkeley, CA 94720.
[2]Present address: Department of Genetics, Harvard Medical School, Boston, MA 02115.
[3]Present address: Department of Chemical and Biomolecular Engineering, University of California, Los Angeles, Los Angeles, CA 90095.
[4]Corresponding author: University of California, Davis, One Shields Ave., Davis, CA 95616-8665. E-mail: wdheyer@ucdavis.edu

key HR functions of homology search and strand invasion, there has been a strong focus on HR regulation at the early stages of Rad51 filament assembly and disassembly. To regulate Rad51 filaments, cells possess protein factors that help stabilize Rad51 filaments as well as factors that help destabilize them (Heyer *et al.* 2010).

Srs2 helicase is a member of the Superfamily 1 UvrD group of DNA helicases conserved from bacteria to mammals (Rong and Klein 1993; Niu and Klein 2017). Srs2 is a paradigmatic antirecombinase that acts by disrupting Rad51 filaments (Krejci *et al.* 2003; Veaute *et al.* 2003). This antirecombination activity of Srs2 is well supported by genetic evidence (Rong *et al.* 1991; Aboussekhra *et al.* 1992; Chanet *et al.* 1996; Fabre *et al.* 2002), as well as biochemical evidence that shows Srs2 can efficiently disrupt Rad51 filaments *in vitro* (Krejci *et al.* 2003; Veaute *et al.* 2003). Single-molecule experiments directly visualized the processive dissociation of Rad51 from ssDNA at a rate of ∼50 Rad51 protomers per second (Kaniecki *et al.* 2017). Efficient Srs2-mediated disruption of Rad51–ssDNA filament requires Rad51 ATPase activity, suggesting that Srs2 directly regulates the Rad51 ATPase (Antony *et al.* 2009; Kaniecki *et al.* 2017). Several biochemical and biophysical studies have shown that blocking the physical interaction between Srs2 and Rad51 prevents Srs2 from efficiently disrupting Rad51 filaments *in vitro* including using the *srs2-Δ(875–902)* mutant protein (Antony *et al.* 2009; Colavito *et al.* 2009; Seong *et al.* 2009; Kaniecki *et al.* 2017). However, genetic and cytological studies of Rad51 interaction-deficient *srs2* mutants such as *srs2-Δ(875–902)* have found no evidence to support the importance of Srs2–Rad51 physical interaction in antirecombination *in vivo* (Colavito *et al.* 2009; Burkovics *et al.* 2013; Sasanuma *et al.* 2013). Despite exhibiting significant defects in Rad51 filament disruption *in vitro*, *srs2-Δ(875–902)* does not suppress *rad18Δ* DNA damage sensitivity (Colavito *et al.* 2009), a genetic interaction that is used as an indirect indicator of defects in Srs2 antirecombination activity. Furthermore, meiotic overexpression of wild type (WT) and *srs2-Δ(875–902)*, unlike helicase-deficient *srs2-K41A*, efficiently removes Rad51 foci from chromosomes, further indicating that the Srs2–Rad51 interaction mediated by Srs2 residues 875–902 may be dispensable for Srs2 antirecombination function *in vivo* (Sasanuma *et al.* 2013). This apparent discrepancy between the *in vitro* and *in vivo* studies may be because of a protein factor/modification missing from the *in vitro* biochemical reactions that is present *in vivo* which may have a greater impact on Srs2 Rad51-filament disruption activity than on the Srs2–Rad51 interaction. One such factor could be Rad52, which is not only required for the nucleation of Rad51 filaments on ssDNA but also to protect Rad51–ssDNA filament against dissociation by Srs2 (Ma *et al.* 2018).

Srs2 has also been shown to promote formation of NCO repair products (Ira *et al.* 2003; Robert *et al.* 2006; Welz-Voegele and Jinks-Robertson 2008; Mitchel *et al.* 2013; Miura *et al.* 2013), at least in part, by unwinding extended D-loops to promote the SDSA subpathway in HR (Liu *et al.* 2017; Piazza *et al.* 2019). One proposed mechanism suggests that Srs2 and other enzymes such as human RECQL5 may promote SDSA through its Rad51 filament disruption activity by removing Rad51 from the second end of the break, thus facilitating the annealing of the newly synthesized strand to the second resected end (Ira *et al.* 2003; Mitchel *et al.* 2013; Paliwal *et al.* 2014). This hypothesis would predict that any mutation that affects the Srs2 antirecombination function would also affect the Srs2 pro-SDSA function. Alternatively, Srs2 pro-SDSA function may rely on another unique biochemical activity separate from its well-characterized Rad51 filament disruption activity. One such activity could be its ability to unwind extended D-loops, which would promote the SDSA pathway and the formation of NCO repair products (Ira *et al.* 2003; Dupaigne *et al.* 2008; Liu *et al.* 2017; Piazza *et al.* 2019).

Here, we identify a putative BRC repeat motif (residues 891–894) within the previously mapped Srs2–Rad51 interaction domain (residues 862–914). We find that mutating F891 within this motif weakens the Srs2–Rad51 physical interaction. Interestingly, *srs2-F891A* promotes a robust shift from NCO to CO repair products in a gap repair assay without any measurable effect on overall repair efficiency. This shift toward CO repair products suggests the *srs2-F891A* mutation may be interfering with the Srs2 pro-SDSA function (Aylon *et al.* 2003; Ira *et al.* 2003; Mitchel *et al.* 2013). However, *srs2-F891A* does not exhibit a shift toward CO repair in an ectopic physical recombination system. Therefore, the *srs2-F891A* mutation interferes with the Srs2 pro-SDSA function only under specific circumstances. Furthermore, despite its weakened interaction with Rad51, *srs2-F891A* does not affect Srs2 antirecombination function as examined both *in vivo* and *in vitro*. Our findings suggest that the *srs2-F891A* mutation, under certain circumstances, selectively disrupts the Srs2 pro-SDSA function without affecting its antirecombination activity, which in turn argues in favor of the idea that the Srs2 pro-SDSA function may be dictated by a biochemical activity separate and unique from its Rad51 filament disruption activity. These findings further highlight the complexity of the Srs2 C-terminal Rad51 interaction domain, suggesting this region includes sites with very specific effects on Srs2 function.

Materials and Methods

Yeast two-hybrid assays

Full-length, WT budding yeast *Srs2* coding DNA was cloned into the yeast 2-hybrid prey vector (pJG4-5) in frame with the B42 activation domain and an HA tag using *Eco*RI and *Xho*I restriction sites. The *srs2-F891A* mutant allele was constructed via site-directed mutagenesis using pJG4-5-Srs2 as a template. Full-length budding yeast *RAD51* was cloned into 2-hybrid bait vector (pEG202) in frame with the LexA domain using *Eco*RI and *Xho*I restriction sites. To prevent translation past the B42 and LexA domains in pJG4-5 and pEG202 negative control vectors, in-frame stop codons were

introduced at the *Eco*RI sites. The list of plasmids used is found in Supplemental Material, Table S1 in File S1.

Budding yeast EGY48 strain (see Table S2 in File S1 for a list of all *Saccharomyces cerevisiae* strains used) was transformed with pSH18-34 LacZ reporter plasmid, as well as prey and bait vectors as indicated in Figure 1C. The resulting strains were grown on selective media and β-galactosidase activity measured in Miller units as previously described (Harshman *et al.* 1988).

DNA damage sensitivity

For the quantitative UV survival assay, yeast strains (Table S2 in File S1) were grown overnight rotating at 30° and then diluted appropriately and plated onto YPD, followed by UV irradiation at the indicated doses (Spectrolinker, XL-1500 UV cross-linker). The plates were incubated at 30° for 2 days. The number of colonies in UV-treated cells was compared to that of untreated controls. For quantitative the gamma-irradiation sensitivity assay, log phase cultures of strains were diluted and plated onto YPD followed by *gamma radiation* from a *cesium*-137 source at the indicated doses. The plates were then incubated for 2 days at 25°. Room temperature (25°) incubation was selected because *rad55Δ* strains are known to be cold-sensitive (Lovett and Mortimer 1987). The number of colonies in gamma-irradiated strains was compared to untreated controls.

For the serial dilution assays, the OD_{600} of overnight yeast cultures was adjusted to 2.0, followed by six fivefold serial dilutions. 2 μl of each dilution was spotted in order onto YPD plates with or without DNA damage induction.

DSB repair efficiency, crossover frequency, and recombination rate analyses

Gap repair, ectopic physical recombination, and spontaneous inverted repeat assays were carried out as previously described (Ira *et al.* 2003; Spell and Jinks-Robertson 2004a; Mitchel *et al.* 2013). To generate the radioactive probe for the ectopic physical recombination assay, the following two primers were used: 5′-TGGATGATATTTGTAGTATGGCGG-3′ and 5′-CCGCATGGGCAGTTTACCT-3′.

Protein purification, affinity pull-down assay, immunoblots

S. cerevisiae His9-tagged wild type and *srs2-F891A* were purified to near homogeneity from *Escherichia coli* (Figure S1 in File S1), and native Rad51 was purified from the cognate host as described (Liu *et al.* 2017). Pull-downs were conducted as previously described with 1.34 μM Rad51 and 0.424 μM His9-tagged Srs2 at the indicated concentrations of KCl (Colavito *et al.* 2009). The resulting eluates were analyzed on 4–20% Mini-PROTEAN TGX Stain-Free Protein Gels (Biorad, Hercules, CA). Srs2 bands were visualized by activating the stain-free gel by exposure to 1 min of UV transillumination with the ChemiDoc Touch (Biorad). Rad51 bands were visualized using immunoblot analysis with rabbit anti-Rad51 serum (a generous gift from Dr. Akira Shinohara). The band intensities were analyzed using ImageJ software.

To examine the interaction between Srs2 and Rad55, 200 nM purified GST–Rad55–His6–Rad57 or 200 nM GST (GE Healthcare) were incubated with 50 nM purified His9-tagged Srs2 (WT or F891A) in buffer K (20 mM potassium phosphate pH 7.4, 10% glycerol, 0.5 mM EDTA, 0.01% NP-40 alternative, 1 mM DTT) with 150 mM NaCl for 1 hr at room temperature. Eighty microliters of preequilibrated and BSA-blocked Glutathione Sepharose 4B bead slurry was added to the protein mixtures and incubated while mixing for an additional 1.5 hr at room temperature. The beads were centrifuged and washed twice with 150 μl of K buffer. The pulled-down protein complexes were eluted off the beads by boiling the beads in 25 μl of 2× Laemmli sample buffer (26.3% glycerol, 65.8 mM Tris-Cl pH 6.8, 2.1% SDS, 0.01% bromophenol blue, 710 mM β-mercaptoethanol) for 5 min. The resulting eluate was loaded on 4–20% Mini-PROTEAN TGX Precast Protein Gels (Biorad). The protein bands were visualized through immunoblot analysis using anti-Srs2 (sc11991; Santa Cruz Biotechnology) and anti-Rad55 (Bashkirov *et al.* 2000) antibodies.

Whole protein was extracted from wild-type, *srs2-F891A*, and *srs2Δ* strains using the trichloroacetic acid (TCA) extraction protocol described in Clontech Yeast Protocols Handbook (Protocol No. PT3024-1, Version No. PR973283). For protein detection by immunoblotting, TCA whole cell extracts were separated by SDS-PAGE and analyzed by immunoblotting using anti-PGK1 (ab197960; Abcam) and anti-Srs2 (sc11991; Santa Cruz Biotechnology) antibodies.

ATPase assay

A coupled spectrophotometric ATPase assay was performed as described previously with minor modifications (Liu *et al.* 2006). Reactions were carried out in 35 mM Tris-acetate pH 7.5, 100 mM NaCl, 7 mM magnesium acetate, 2 mM ATP, 1 mM DTT, 0.25 mg/ml BSA, and an ATP regenerating system [30 U/ml pyruvate kinase (Sigma, St. Louis, MO), 3 mM phosphoenolpyruvate (Sigma), and 0.3 mg/ml NADH (Sigma)], in the presence or absence of 10 μM (in nucleotides) ϕX174 ssDNA cofactor. Purified Srs2 WT or F891A (5 nM) was added to initiate the reactions at 30°. ATP hydrolysis rates were estimated from the measured changes in absorbance at 340 nm within the linear portions of time courses.

D-loop disruption assay

The D-loop disruption assay was carried out as recently described (Liu *et al.* 2017).

Assay for Rad51 filament disruption

A 5′-biotinylated 100-mer with sequence 5′-ATGTCTAA TATTCAAACTGGCGCCGAGCGTATGCCGCATGACCTTTCC CATCTTGGCTTCCTTGCTGGTCAGATTGGTCGTCTTATTAC CATTTCAACTA-3′ was immobilized onto magnetic streptavidin beads (M-280; Thermo Fisher) as described by Liu *et al.* (2011). Two μl of suspended beads were incubated

with 1 μM nucleotides ssDNA and agitated with 300 nM Rad51 in 10 μl reaction buffer (35 mM Tris-acetate, 7 mM magnesium acetate, 4 mM ATP, 50 μg/ml BSA, and 1 mM DTT) for 20 min. Beads were washed with reaction buffer to remove free Rad51. Beads were then agitated with 10 μl of reaction buffer with or without 25 nM Srs2 or Srs2-F891A for 20 min. Nucleotides (100 μM) of noncomplementary scavenger DNA with the sequence 5′-CTTGCTGAATA TATCTGGAAGTATTATGCAGATTCATTATTCGAAGGGGGAGG CGGGGGTGGAAAGCCTATCCCTAACCCTCTCCTCGGTCTC GATTCTA-3′ were added and further incubated for 10 min. Supernatant containing unbound proteins was collected and tested for the amount of Rad51 by immunoblot analysis with mouse anti-Rad51 (sc-133089; Santa Cruz Biotechnology) antibody using a 1:500 dilution. All steps were carried out at 30°.

Data availability

Strains and plasmids are available upon request. Table S1 lists the two-hybrid plasmids used. Table S2 lists the *S. cerevisiae* strains used. Figure S1 shows the purified Srs2-F891A protein. Figure S2 shows the Srs2-Rad55 interaction data. Figure S3 shows ATPase data. Figure S4 shows DNA damage sensitivity data. Figure S5 shows tetrad data for absence of synthetic lethalities. Supplemental material available at FigShare: https://doi.org/10.25386/genetics.8179493.

Results

The Rad51 interaction domain of Srs2 contains a BRC repeat motif

Human RECQL5, a potential functional homolog of yeast Srs2, was previously proposed to possess a BRC repeat motif mediating its interactions with Rad51 much like the interaction between BRCA2 and Rad51 (Islam *et al.* 2012). In fact, the authors also reported finding BRC repeat-like motifs in other known yeast HR proteins such as Srs2, Mph1, Sgs1, and Pif1 (Islam *et al.* 2012). The Srs2 BRC repeat motif previously proposed by Islam *et al.* (2012) spans amino acids 837 through 840 (FTAA). However, srs2-F837A mutant protein exhibited no Rad51 interaction defect, even though, at low concentrations, it exhibited a slight decrease in inhibiting D-loop formation *in vitro* (Islam *et al.* 2012). This prompted us to look further within the Srs2 sequence for other potential BRC repeat motifs. We particularly focused our search on amino acids 875 through 902, a region whose deletion (*srs2-Δ(875–902)*) has been shown to effectively disrupt Srs2–Rad51 physical interaction *in vitro* (Colavito *et al.* 2009). We identified residues 891–894, FHSP, as a potential BRC repeat motif (Figure 1A). Even though BRC repeat motifs typically have an alanine at the fourth site, there is precedence for a proline at this position in the *Gallus gallus* BRC5 repeat motif (Warren *et al.* 2002) (Figure 1B).

srs2-F891A exhibits reduced interaction with Rad51

Crystallographic data have shown that the phenylalanine in a BRC repeat functions as a hydrophobic key that is wedged into a hydrophobic Rad51 pocket (Pellegrini *et al.* 2002). We, therefore, mutated F891 to alanine to eliminate this potential hydrophobic interaction without significantly altering the overall charge and polarity. We used yeast 2-hybrid assays to examine how the predicted BRC repeat region affects the Srs2–Rad51 interaction. The analysis shows that mutating F891 to alanine greatly reduces the interaction between Srs2 and Rad51 (Figure 1C). To further examine the Rad51 interaction defect conferred by the *srs2-F891A* mutation, we purified His9-tagged WT Srs2 and Srs2-F891A from *E. coli* to near homogeneity (Figure S1 in File S1) and tested the physical interaction with Rad51 (Figure 1D). We found that compared to WT Srs2, srs2-F891A showed a consistent decrease in Rad51 interaction *in vitro* over a range of salt concentrations (Figure 1D).

To verify that the *srs2-F891A* mutation does not cause overall misfolding that blocks all protein interactions, we tested its interaction with another known Srs2 interacting protein, Rad55 (Liu *et al.* 2011). We found that Srs2-F891A is just as adept as WT Srs2 in interacting with Rad55 (Figure S2 in File S1) at a salt concentration (150 mM) that caused a significant reduction in Rad51 interaction with Srs2-F891A (Figure 1D). The intact Srs2-F891A-Rad55 interaction indicates that this mutant Srs2 is not grossly misfolded.

To further assess whether Srs2-F891A mutation affects protein folding and stability, we compared its endogenous protein expression levels to that of wild-type Srs2. Generally, misfolded proteins are associated with a reduction in protein stability that translates into lower steady-state protein levels. We found WT Srs2 and Srs2-F891A are expressed to the same steady-state level, further indicating Srs2-F891A mutant protein is properly folded (Figure 2D).

In accordance with these findings, purified mutant Srs2-F891A protein exhibits levels of ATPase activity comparable to that of WT Srs2 (Figure S3 in File S1).

srs2-F891A mutant is proficient at antirecombination in vivo

The observation that Srs2-F891A is defective in Rad51 interaction would suggest that it is also defective in Rad51 filament disruption, and consequently, antirecombination. To investigate the antirecombination effects of the *srs2-F891A* mutation *in vivo*, we examined sensitivity of the mutant to various DNA-damaging agents. The *srs2-F891A* mutant displayed no statistically significant or reproducible sensitivity to ultraviolet light (UV), ionizing radiation (IR), or methyl methanesulfonate (MMS) beyond that observed in WT strains (Figure 2, A–C and Figure S4 in File S1). Moreover, we investigated its genetic interactions with *rad55Δ* and *rad18Δ*, whose DNA damage sensitivity is suppressed by *srs2Δ* (Lawrence and Christensen 1979; Rong *et al.* 1991; Liu *et al.* 2011). The observed suppression in the double deletion mutants, *srs2Δ rad55Δ* and *srs2Δ rad18Δ*, are attributed to loss of Srs2 antirecombination activity. While the *srs2Δ* mutation partially suppressed the *rad55Δ* IR sensitivity

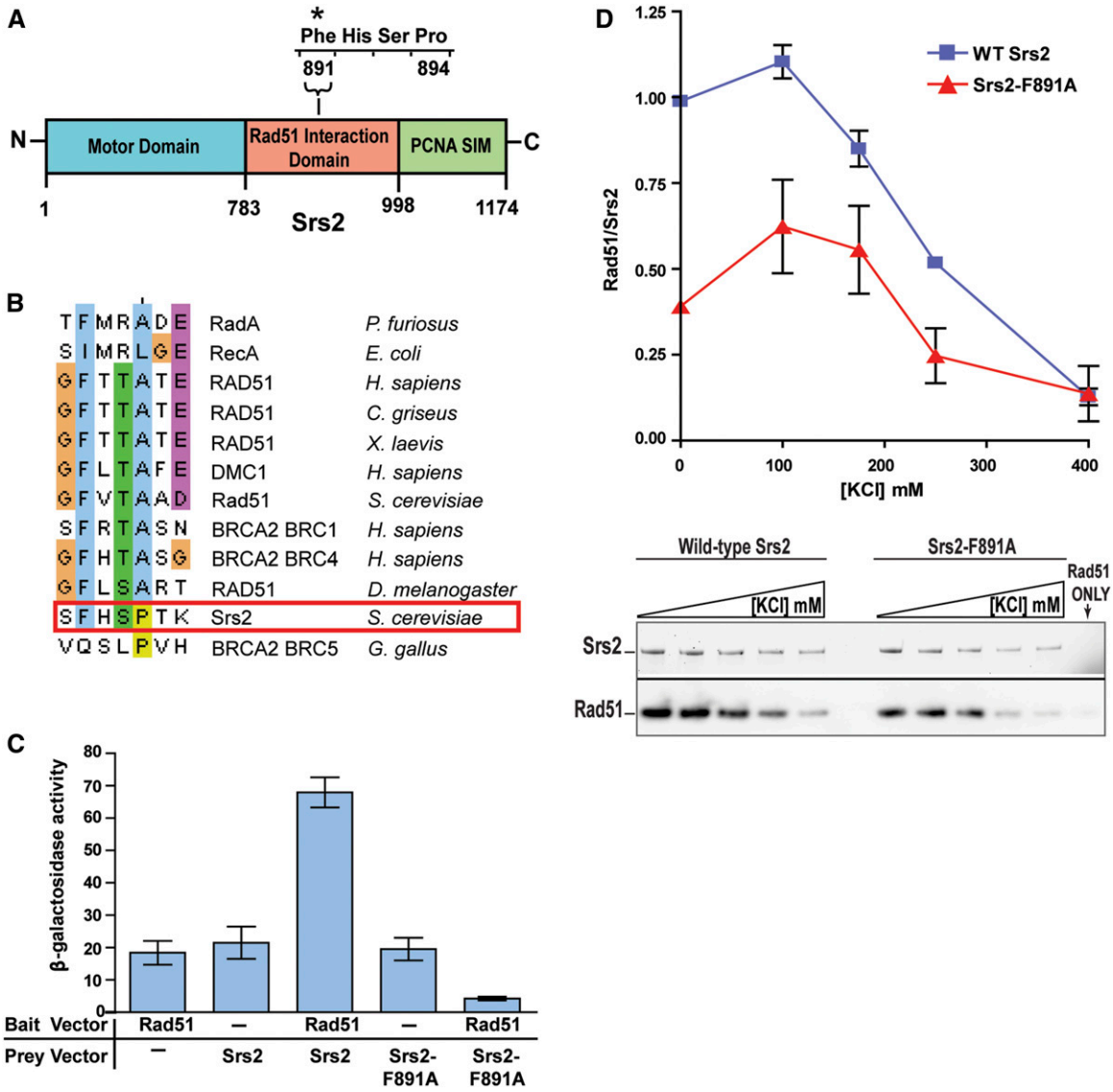

Figure 1 Mutations targeting the putative Srs2 BRC repeat-like motif weaken the Srs2–Rad51 physical interaction. (A) Schematic of Srs2 domains. (B) Sequence alignment of the putative Srs2 BRC repeat motif with other BRC repeat motifs in the indicated species. Glycine (G): orange; phenylalanine (F), isoleucine (I), leucine (L), alanine (A): blue; serine (S), threonine (T): green; proline (P): yellow; aspartic acid (D), glutamic acid (E): violet. (C) Quantitative β-galactosidase assay analyzing the physical interaction between full-length Srs2 and Rad51. (D) Ni-NTA pull-down with 1.3 μM Rad51 and 0.4 μM His9-tagged Srs2 (WT or srs2-F891A) at increasing concentrations of KCl (0–400 mM). Srs2 was visualized using a Biorad stain-free imaging system. Rad51 bands were detected by immunoblot analysis. The amount of Rad51 pulled down was normalized against the amount of Srs2 pull-down in each lane. Shown are means ±1 SE, n = 2–3.

as expected (Liu *et al.* 2011), we observed no suppression of *rad55Δ* IR sensitivity in *srs2-F891A* mutant background (Figure 2B), further suggesting that *srs2-F891A* is proficient at antirecombination *in vivo*.

Early studies showed that *srs2* suppresses the DNA damage sensitivities of *rad6* and *rad18* mutants (Lawrence and Christensen 1979; Rong *et al.* 1991), which represents the key phenotype of its antirecombination activity. Rad18 is an E3 ubiquitin ligase that forms a functional complex with Rad6, an E2 ubiquitin-conjugating enzyme. The Rad6-Rad18 complex ubiquitylates PCNA; the ubiquitylated PCNA, in turn, recruits translesion synthesis (TLS) polymerases to bypass damaged nucleotides (Hoege *et al.* 2002; Bienko *et al.* 2005). As expected, mutations affecting *RAD18* or *RAD6* exhibit significant DNA damage sensitivity. *srs2Δ* suppresses both *rad6* and *rad18* damage sensitivity by allowing HR-mediated repair to be substituted for TLS-mediated DNA damage tolerance. We hypothesized that if *srs2-F891A* mutation affected the Srs2 antirecombination activity, then *srs2-F891A* should also suppress *rad18Δ* MMS sensitivity. Based on our findings, however, *srs2-F891A* does not suppress *rad18Δ* DNA damage sensitivity, further supporting the idea that this mutant is proficient at antirecombination (Figure 2C).

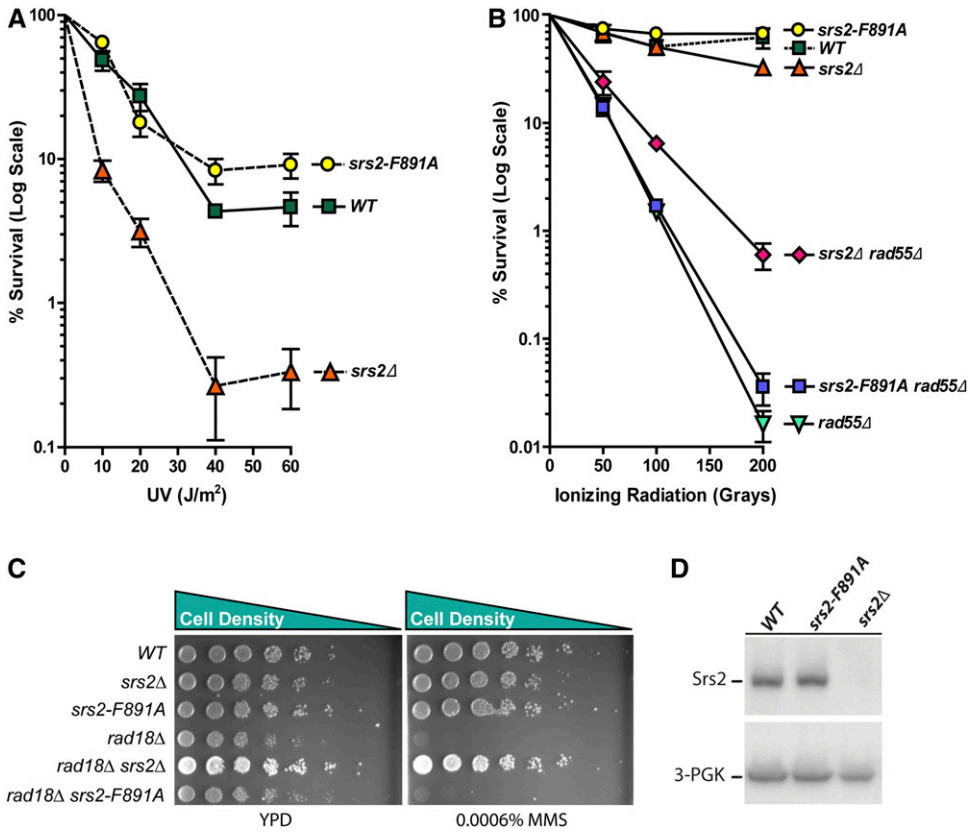

Figure 2 *srs2-F891A* mutation has no effect on UV sensitivity, *rad55Δ* IR sensitivity, or *rad18Δ* MMS sensitivity. (A) Quantitative UV survival assay. The indicated haploid W303 strains were grown to stationary phase in liquid YPD medium, plated onto YPD, UV irradiated, and then grown at 30° for 2 days. The number of surviving colonies was normalized to the number of viable colonies in the unirradiated control samples. (B) Quantitative IR survival assay. The indicated haploid W303 strains were grown to midlog phase, irradiated with IR (0–200 Gy), and then plated onto YPD and grown at 25° for 2 days. *srs2-F891A*, unlike *srs2Δ*, does not suppress *rad55Δ* IR sensitivity. (C) Qualitative MMS survival assay. Strains were grown to stationary phase in liquid YPD. Serial fivefold dilutions of the strains were then spotted onto YPD or 0.0006% MMS and grown at 30° for 1 day. The *srs2Δ rad18Δ* double mutant appears white because it is *ADE2+* unlike the other strains depicted. *srs2Δ* suppresses *rad18Δ* MMS sensitivity as expected. (D) Immunoblot analysis of whole cell protein TCA extraction of WT and *srs2-F891A* strains (W303 background). *srs2Δ* was used as a negative control. Shown are means ±1 SE, $n = 3$.

In addition to damage sensitivity, we also investigated *srs2-F891A* genetic interactions with *sgs1Δ* and *rad54Δ*, which exhibit synthetic growth defect and synthetic lethality with *srs2Δ*, genetic interactions linked to loss of Srs2 antirecombination function. These negative genetic interactions have been attributed to the accumulation of toxic recombination intermediates due to the absence of the Srs2 antirecombinase activity (Palladino and Klein 1992; Gangloff *et al.* 2000). Neither *rad54Δ srs2-F891A* nor *sgs1Δ srs2-F891A* double mutants exhibit any synthetic lethality or growth defects (Figure S5 in File S1).

srs2-F891A mutant is proficient at antirecombination in vitro

The importance of Srs2–Rad51 interaction in Srs2 antirecombination activity has primarily been demonstrated *in vitro* and not *in vivo*. Several studies have shown that blocking the Srs2–Rad51 interaction prevents Srs2 from disrupting Rad51 filaments *in vitro* (Antony *et al.* 2009; Colavito *et al.* 2009; Seong *et al.* 2009). We, therefore, tested whether Srs2-F891A would exhibit a similar defect in Rad51 filament disruption *in vitro*. We examined the Rad51 filament disruption activity of Srs2-F891A *in vitro* using magnetic beads coupled with ssDNA and bound by Rad51 (Figure 3A) (Islam *et al.* 2012). Addition of either Srs2 or Srs2-F891A was associated with a comparable increase in the amount of Rad51 bound to scavenger DNA, indicative of no defect in Rad51 filament disruption with Srs2-F891A (Figure 3, B and C).

In summary, both our genetic and biochemical observations suggest *srs2-F891A* is proficient at antirecombination both *in vivo* and *in vitro* despite the observed decrease in its Rad51 interaction.

srs2-F891A exhibits a shift from NCO to CO repair products in plasmid-based gap repair

The Srs2 antirecombinase activity has been shown to be dependent on the Srs2–Rad51 physical interaction, particularly *in vitro* (Antony *et al.* 2009; Colavito *et al.* 2009; Seong *et al.* 2009). However, other studies have also shown Srs2 to play an important role in CO control (Aylon *et al.* 2003; Ira *et al.* 2003; Robert *et al.* 2006; Dupaigne *et al.* 2008; Mitchel *et al.* 2013; Miura *et al.* 2013). Interestingly, more recently, the Srs2–Rad51 physical interaction has also been implicated in regulating SDSA-mediated repair (Miura *et al.* 2013). Removal of Srs2 amino acid residues 860 through 998, a deletion that is expected to disrupt the Srs2–Rad51 interaction, results in a subtle but statistically significant increase in SDSA repair efficiency in a plasmid-based repair assay (Colavito *et al.* 2009; Miura *et al.* 2013). Conversely, however, deletion of Srs2 amino acids 783–998 or 783–859, deletions also predicted to disrupt Rad51 interaction, significantly *decreases* SDSA repair (Krejci *et al.* 2003; Miura *et al.* 2013). Despite the conflicting results

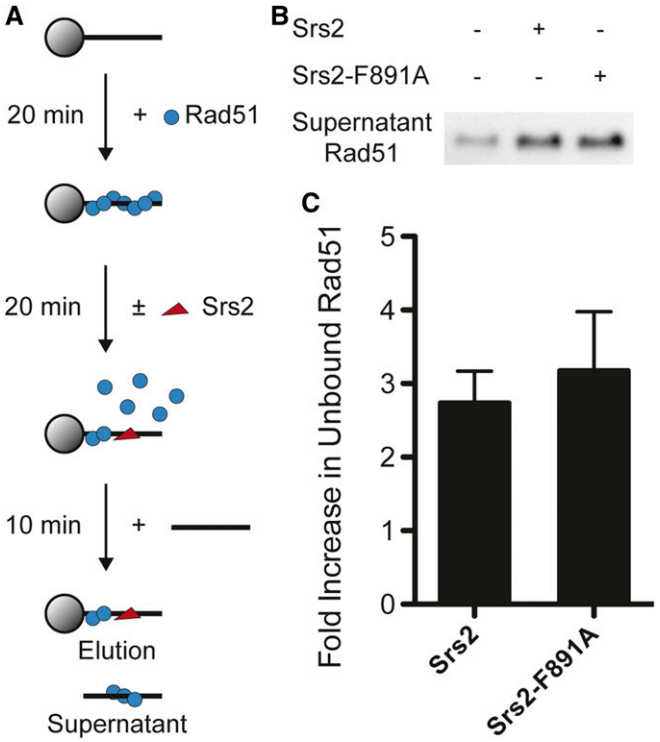

Figure 3 Srs2-F891A and Srs2 disrupt Rad51 filaments at similar rates. *In vitro* disruption of Rad51 filaments. (A) A schematic of the assay where Rad51 filaments were assembled on ssDNA immobilized to magnetic beads and disrupted by Srs2 or Srs2-F891A. (B) Supernatant Rad51 bound to scavenger DNA with 25 nM of Srs2 or Srs2-F891A was analyzed by immunoblot. A representative blot is shown. (C) Quantification of supernatant Rad51 was normalized to fold increase over no Srs2 added. Shown are means ±1 SD, $n = 3$. The difference is not significant by a Student's *t*-test.

with the different Srs2 internal deletions, these findings suggested that the Srs2–Rad51 interaction region also plays a role in SDSA regulation. Given the reduced Rad51 interaction observed with Srs2-F891A, we were particularly interested in examining how *srs2-F891A* mutation might affect the Srs2 pro-SDSA function.

To assess SDSA in *srs2-F891A*, a previously developed plasmid-based gap repair assay was employed to determine whether *srs2-F891A* affects repair efficiency and CO to NCO ratios in a manner similar to *srs2Δ* (Figure 4A) (Mitchel *et al.* 2010, 2013). The gap repair assay relies on the transformation of a linearized *URA3* ARS plasmid missing 8 bp from the middle of the 800-bp *HIS3* marker. A chromosomally integrated *his3* mutant allele with the last 11 codons missing is used as a repair template for the linearized plasmid. If the plasmid is repaired without associated CO events, then the plasmid is not integrated and thus, in the absence of selection, the *URA3* marker will persist only temporarily. However, if the plasmid repair is associated with a CO event, then the plasmid will be chromosomally integrated, thus leading to stable maintenance of the *URA3* marker. This gap repair system examines the frequency of His^+ transformants, indicative of overall repair efficiency and CO to NCO ratios, by measuring the fraction of His^+ transformants that possess a stable *URA3* marker. *srs2Δ* showed a reduction in overall repair efficiency as previously reported (Mitchel *et al.* 2013), but *srs2-F891A* mutants did not exhibit a significant change in overall gap repair efficiency (Figure 4, B and C). The *srs2-F891A* mutant did, however, display a statistically significant shift from NCO to CO repair products in two different strain backgrounds (W303 and SJR; Figure 4, B and C). It is important to note that the increase in CO frequency is not the result of lower Srs2-F891A protein levels (Figure 2D). The CO to NCO ratios observed in the *srs2-F891A* mutant closely resemble the ratios observed in *srs2Δ*, even though *srs2-F891A*, unlike *srs2Δ*, exhibits no measurable defect in overall repair efficiency. This observation suggests the *srs2-F891A* mutation specifically disables Srs2 pro-SDSA activity while leaving its antirecombination activity intact. This apparent separation-of-function mutation suggests that the Srs2 pro-SDSA function may be independent of its well-documented Rad51 filament disruption activity. This finding also suggests that the Srs2-F891 residue mediating Rad51 interaction may play a role in the Srs2 pro-SDSA function.

Yeast Mph1 helicase, an ortholog of the human FANCM, has been shown to promote an NCO outcome, likely through its D-loop disruption activity observed *in vitro* (Prakash *et al.* 2009). We reasoned that if Srs2 and Mph1 have partially overlapping functions, then *mph1Δ srs2-F891A* double mutants might exhibit a greater shift toward CO repair products than the single mutants. To test this, we examined the genetic interaction between *mph1Δ* and *srs2-F891A* in the gap repair system. *srs2Δ mph1Δ* double mutants were excluded from the genetic analyses, because of their severe synthetic growth defects and poor spore viability (Tong *et al.* 2004; Chen *et al.* 2009; Prakash *et al.* 2009; Panico *et al.* 2010). Similarly to *srs2-F891A*, earlier studies showed that an *mph1Δ* mutant exhibits no gap repair deficiency despite a clear shift from NCO to CO repair products (Mitchel *et al.* 2013). Our direct comparison of the two mutants in the W303 background confirms this observation (Figure 4B). Contrary to our expectation, the *srs2-F891A mph1Δ* double mutants exhibited no increased shift toward CO repair products beyond that observed in either single mutant (Figure 4B). However, the double mutants did have a synergistic defect in overall gap repair efficiency indicative of a genetic interaction between *srs2-F891A* and *mph1Δ* (Figure 4B). *srs2-F891A* and *mph1Δ* did not exhibit any synergistic survival defects in response to IR, UV, or MMS (Figure S4 in File S1). It is important to note that the gap repair assay used here is limited to analyzing repair products among the surviving cells. Therefore, it is possible that CO events may be disproportionately represented among dying cells, which may explain why the *srs2-F891A mph1Δ* double mutants do not show the expected synergistic increase in CO frequency. Altogether, our findings suggest that while Srs2–Rad51 physical interaction as

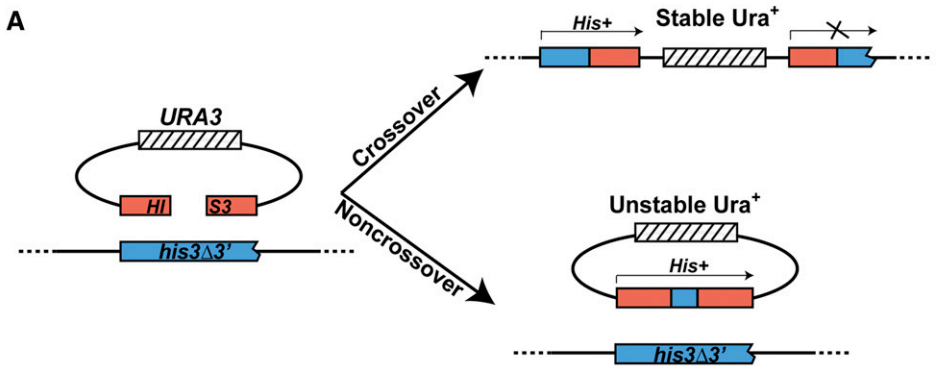

B

Relevant genotype	Plasmid repair efficiency	CO events		NCO events	
W303		**Proportion (%)**	**Efficiency**	**Proportion (%)**	**Efficiency**
WT	1.00 (N=11)	21/190 (11%)	0.11	169/190 (89%)	0.89
srs2-F891A	0.92 (N=12)	41/190 (22%)	0.20*	149/190 (78%)	0.72*
mph1Δ	0.95 (N=12)	55/190 (29%)	0.27*	135/190 (71%)	0.67*
srs2-F891A mph1Δ	0.64* (N=12)	40/190 (21%)	0.14*	150/190 (79%)	0.51*
srs2Δ	0.48* (N=12)	41/190 (22%)	0.10	149/190 (78%)	0.38*

C

Relevant genotype	Plasmid repair efficiency	CO events		NCO events	
SJR		**Proportion (%)**	**Efficiency**	**Proportion (%)**	**Efficiency**
WT	1.70 (N=6)	9/96 (9 %)	0.15	87/ 96 (91 %)	1.55
srs2-F891A	1.57 (N=6)	20/96 (21 %)	0.33*	76/ 96 (79 %)	1.24 *

Figure 4 *srs2-F891A* (W303 strain background) increases the relative CO frequency without affecting overall repair efficiency. (A) Schematic of the gap repair system. Plasmid linearized within the *HIS3* reading frame was transformed into yeast strain where *his3Δ3′* serves as the repair template for the linearized plasmid. The stable presence of the *URA3* marker was used as an indicator of plasmid integration, representing CO events, while the unstable presence of the *URA3* marker was used an indicator of plasmid repair without integration, representing NCO events. (B) Gap repair assay shows that *srs2-F891A* (W303 strain background) has no defect in repair efficiency but exhibits a clear shift from NCO repair products to CO repair products similar to *srs2Δ*. All strains were MMR-defective (*mlh1Δ*). Asterisks indicate a significant difference when compared to WT using a Student's *t*-test ($P \leq 0.05$). (C) Gap repair analysis of *srs2-F891A* in SJR strain background recapitulates findings in the W303 strain background.

mediated by Srs2-F891 residue is not critical for the Srs2 antirecombination function, it may play an important role in SDSA/CO regulation in plasmid-based gap repair.

srs2-F891A exhibits wild-type NCO to CO ratios in an ectopic physical assay

To confirm the plasmid-based gap repair findings and to better evaluate the state of repair among the nonsurviving cell populations, we used a previously designed ectopic physical recombination assay with 1.9-kb homology of 1.4 and 0.5 kb flanking the DSB (Figure 5A) (Ira *et al.* 2003). We reproduced earlier findings showing an increase in CO frequency in *srs2Δ* and *mph1Δ* mutants (Ira *et al.* 2003; Xue *et al.* 2016). Surprisingly, this chromosome-based physical assay did not detect a measurable increase in CO frequency in the *srs2-F891A* mutant (Figure 5, B and C). Even the *srs2-F891A mph1Δ* double mutant did not exhibit any further increase in CO frequency compared to that observed in the *mph1Δ* single mutant (Figure 5, B and C). In conclusion, even though the *srs2-F891A* mutants in both W303 and SJR yeast strain backgrounds showed a clear and reproducible shift from NCO to CO repair products in the plasmid-based gap repair assay, the ectopic physical recombination assay did not detect a similar effect.

srs2-F891A is proficient at spontaneous inverted repeat recombination

Since the physical recombination assay, unlike the plasmid-based gap repair assay, did not produce a phenotype for *srs2-F891A*, we hypothesized the different outcomes in the two assays may be linked to the variable extents of sequence homology. Therefore, we tested the effects of the *srs2-F891A* mutation in a previously designed intron-based spontaneous inverted repeat assay that provides limited sequence homology (783 bp) and has previously detected a robust increase in recombination rate in *srs2Δ* mutants (Figure 6A) (Spell and Jinks-Robertson 2003, 2004b). We compared the recombination rates of WT, *srs2Δ*, and *srs2-F891A* in the inverted repeat assay. We detected a robust, eightfold increase in *srs2Δ* recombination rates as previously reported; however, the *srs2-F891A* mutation did not significantly increase recombination rates (Figure 6B). This result confirms the retention of antirecombination activity in the *srs2-F891A* mutant but does not provide insight into the differences between the gap repair and physical assays.

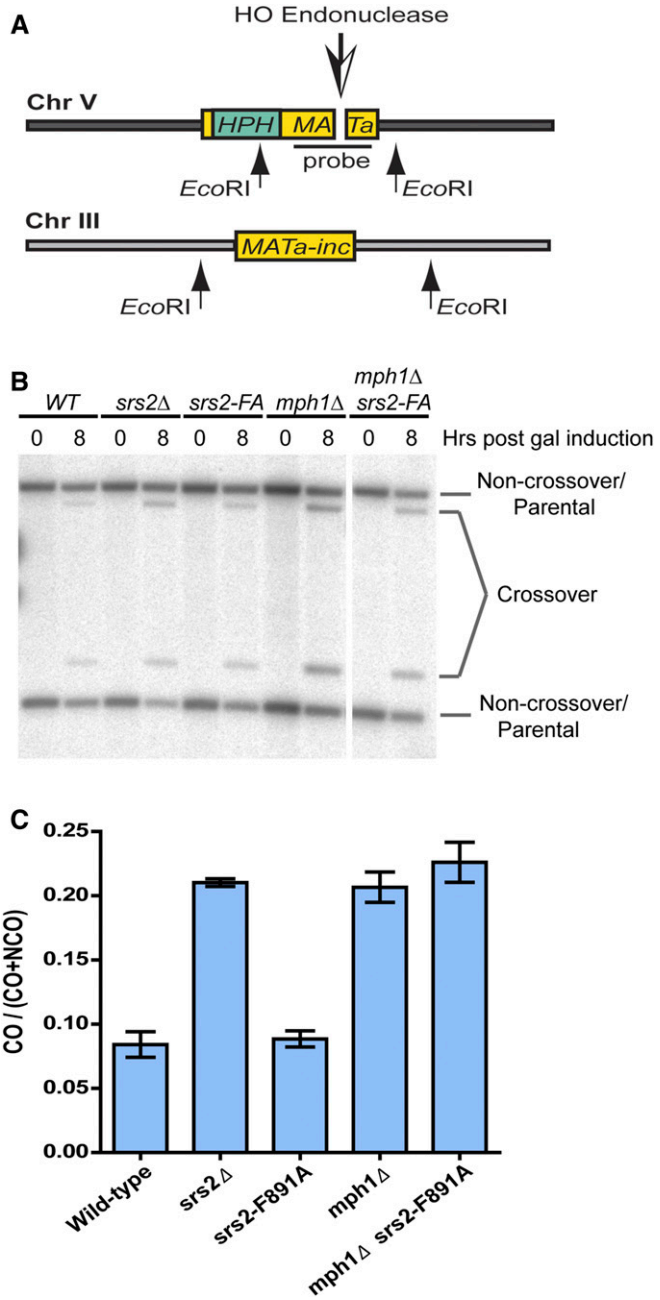

Figure 5 Ectopic physical recombination assay. (A) Schematic of the ectopic physical recombination assay. (B) Representative Southern blot analysis of the CO and NCO repair products for the strains shown in the figure. (C) Quantitative analysis of the CO to NCO ratio. The lower CO band intensities were divided by the sum of the lower CO and NCO bands. In contrast to the gap repair system, the ectopic physical recombination assay does not exhibit a shift from NCO to CO repair products even in an *mph1Δ* background. Shown are means ±1 SE, $n = 3$.

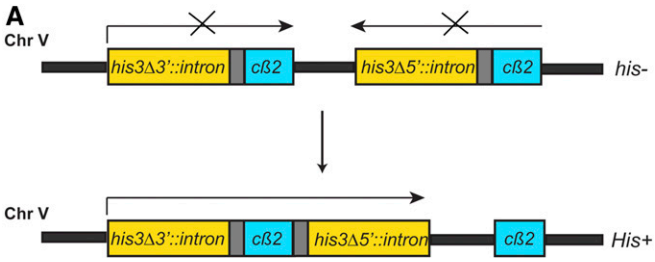

B

Relevant Genotype	Rate x 10^{-8}		Relative Rate
Wild-type	147	(123-161)	1.0
srs2Δ	1240	(960-1594)	8.4
srs2-F891A	172	(148-249)	1.2

95% confidence intervals are indicated in the parentheses.

Figure 6 Spontaneous inverted repeat assay. (A) Schematic of the intron-based inverted repeat recombination assay. Inverted repeats of cβ2 intron sequence (blue) are fused to intron splice sites (gray) positioned adjacent to the 5′ and 3′ halves of the *HIS3* gene (yellow). Spontaneous CO events at cβ2 intron sequence reorient and bring together the *his3* halves. The resulting transcript produces a functional HIS3 mRNA after splicing out the cβ2 intervening sequence. (B) Recombination rates for wild type and *srs2Δ* recapitulate findings previously published (Spell and Jinks-Robertson 2003, 2004b). *srs2-F891A* mutant exhibits rates of recombination comparable to that of the wild type.

Srs2-F891A is proficient at dissolving stable Rad51-catalyzed D-loops in vitro

Given that *srs2-F891A* exhibited a robust shift toward CO repair products in the plasmid-based gap repair assay while maintaining intact antirecombination activities, we hypothesized that *srs2-F891A* may be specifically disabled in D-loop disruption, an activity which has only recently been observed *in vitro* (Liu *et al.* 2011). To address this possibility, we reconstituted Rad51-catalyzed D-loops *in vitro* and challenged them with increasing concentrations of both WT and Srs2-F891A mutant protein (Figure 7A). Surprisingly, despite the robust shift in favor of CO repair in the plasmid-based repair assay, the Srs2-F891A mutant protein showed no significant defect in D-loop disruption *in vitro* (Figure 7, B and C).

Discussion

Srs2-mediated Rad51 filament disruption/antirecombination has long been proposed to require a physical interaction with Rad51. This notion is largely supported by extensive biochemical studies which have shown that Rad51 interaction-deficient *srs2* mutants (C-terminal or internal deletions) are also deficient in Rad51 filament disruption *in vitro*. However, genetic analyses of such Rad51 interaction-deficient *srs2* mutants are limited. Studies that have genetically and cytologically examined Rad51 interaction-deficient *srs2* mutants with small internal deletions have found little evidence for antirecombination defects *in vivo* (Colavito *et al.* 2009; Burkovics *et al.* 2013; Sasanuma *et al.* 2013). By contrast, C-terminal deletions of Srs2 that remove the Rad51 interaction domain do exhibit antirecombination defects in genetic analyses. These defects, however, are likely because of the simultaneous deletion of the Srs2 PIP-like motif (PCNA-interacting protein box spanning residues 1148–1161) as well as the Srs2 SIM (Sumo interaction motif spanning residues 1168–1174) (Colavito *et al.* 2009; Armstrong *et al.* 2012). To further examine the biological significance of the

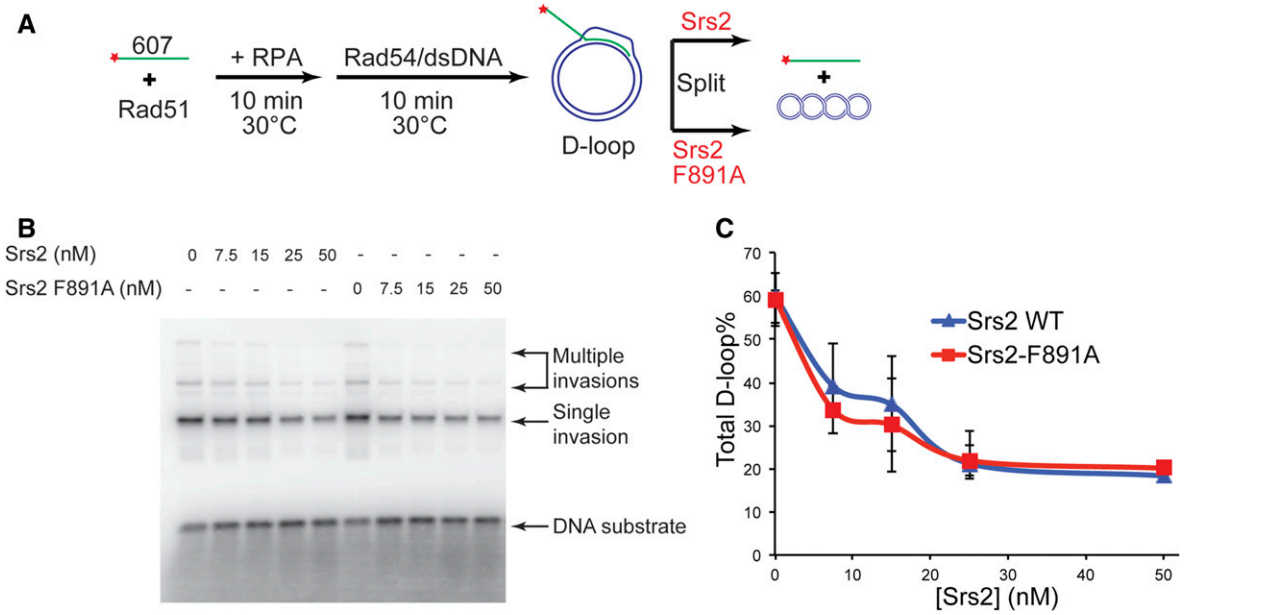

Figure 7 Both Srs2-F891A and Srs2 dissolve the D-loop *in vitro*. (A) Schematic of the reconstituted D-loop disruption assay. (B) Representative gel of Srs2 and Srs2-F891A titration in D-loop disruption assay. (C) Quantification of D-loops in the presence of increasing concentrations of Srs2 and Srs2-F891A proteins. Shown are means ±1 SD, $n = 3$.

Srs2–Rad51 physical interaction, we identified and constructed a single point mutation in the *Srs2* C-terminal Rad51 interaction region (*srs2-F891A*) that measurably reduces Rad51 binding *in vivo* and *in vitro*. Importantly, the *srs2-F891A* mutation, unlike the C-terminal and internal *srs2* deletion mutations examined previously, appears to retain the overall integrity of the protein with minimal effects on other potential Srs2 functions, therefore reducing the likelihood of introducing confounding variables.

Based on our findings, Srs2-F891A, despite its weakened interaction with Rad51, does not exhibit defects in antirecombination in genetic analyses or when using *in vitro* assays. Our *in vivo* findings are consistent with the previous genetic analyses of Rad51 interaction-deficient *srs2* mutants (Colavito *et al.* 2009; Burkovics *et al.* 2013; Sasanuma *et al.* 2013). However, our *in vitro* findings are more surprising and are discussed below.

Other groups have examined the role of the Srs2–Rad51 interaction domain with respect to antirecombination *in vivo*. One study previously showed that deletion of a small region in Srs2 (residues 875–902) effectively blocks interactions with Rad51 (Colavito *et al.* 2009). It further showed that purified Srs2-Δ(875–902) is unable to disrupt Rad51 filaments. However, even though their biochemical findings clearly showed a strong decrease in the Rad51 filament disruption activity of this Srs2 mutant, the authors found *srs2-Δ(875–902)* does not suppress the *rad18Δ* MMS or UV sensitivity (Colavito *et al.* 2009; Burkovics *et al.* 2013). The suppression of the *rad18Δ* DNA damage sensitivity by *srs2Δ* has been attributed to loss of the Srs2 antirecombination function such that Rad51-mediated repair can take the place of the Rad18-mediated postreplicative repair (Lawrence and Christensen 1979; Aguilera and Klein 1988; Aboussekhra *et al.* 1989; Schiestl *et al.* 1994). To explain this inconsistency, the authors hypothesized that *srs2-Δ(875–902)* failed to suppress *rad18Δ* DNA damage sensitivity because Srs2-Δ(875–902) mutant protein may still maintain residual interaction with Rad51. Another group also investigated the *srs2-Δ(875–902)* mutant in their cytological analyses and found that overexpression of Srs2-Δ(875–902) during meiosis still effectively removed Rad51 foci *in vivo* (Sasanuma *et al.* 2013). The results reported here also suggest that the Srs2–Rad51 interaction as mediated through Srs2 residue F891 may be dispensable for Srs2-mediated antirecombination *in vivo*. The apparent discrepancy between the *in vivo* and *in vitro* roles of the Srs2–Rad51 interaction may be because *in vivo* there are other factors, such as PCNA, that are equally, if not more, important for the recruitment of Srs2 for Rad51 filament disruption. In fact, a recent genetic study on *SRS2* concluded that the main role of Srs2 in DNA repair depends on its helicase/translocase activity instead of its Rad51or PCNA interaction (Bronstein *et al.* 2018).

While *in vivo* evidence supporting the biological significance of Srs2–Rad51 interaction in antirecombination is lacking, there is extensive biochemical evidence that shows this interaction is required for Rad51 filament disruption *in vitro* (Antony *et al.* 2009; Colavito *et al.* 2009). Therefore, the robust Rad51 filament disruption activity of *srs2-F891A in vitro* was surprising. Several studies have examined various C-terminal deletions or small internal deletions of Srs2 that abrogate its interaction with Rad51 and have found these mutant Srs2 proteins to be defective in Rad51 filament disruption *in vitro* (Antony *et al.* 2009; Colavito *et al.* 2009; Seong *et al.* 2009). This contrasts with our findings for

Srs2-F891A. However, in contrast to the Srs2-F891A point mutant, these mutants involve deletions of at least 27 residues, which are expected to have more extensive effects on Srs2 function. Therefore, it is possible that the previous Rad51 interaction-deficient *srs2* mutants, given their larger deletion sizes, have more wide-ranging effects on Srs2 activity.

Only one other study has explored an *srs2* single mutation (L844A) that measurably interferes with Srs2–Rad51 interaction; however, Srs2-L844A, unlike Srs2-F891A, was shown to exhibit reduced Rad51 filament disruption compared to WT Srs2, as extrapolated from D-loop assays (Islam *et al.* 2012). Others have previously proposed that the Srs2–Rad51 interaction is likely mediated by Srs2 residues clustered in separate regions within Srs2 residues 783–998 (Keyamura *et al.* 2016). It is also possible that these separate Rad51 interaction regions affect different aspects of Srs2 function, with the region around L844 mediating Srs2 anti-recombination and the region around F891 mediating Srs2 pro-SDSA function.

As discussed earlier, the Srs2–Rad51 interaction has been implicated in SDSA regulation (Miura *et al.* 2013). In studies by Miura *et al.* SDSA repair efficiency was assayed in a gap repair assay that requires the invasion of two distinct ectopic donor alleles, thus limiting repair to SDSA (Miura *et al.* 2013). Interestingly, the authors showed that *srs2-Δ(860–998)* results in an increase in the overall efficiency of gap repair, interpreted as an *increase* in SDSA-mediated repair (Miura *et al.* 2013). This may appear in conflict with our findings which show that *srs2-F891A* mutation, which falls within the same deleted region, *decreases* SDSA-mediated repair. However, given the size of the deletion in the earlier study, one cannot assume that *srs2-Δ(860–998)* disables only the Srs2–Rad51 interaction without affecting other functions. In fact, this deletion mutation may have also removed a region that is responsible for negatively regulating the pro-SDSA functions of Srs2, leading to the reported increase in SDSA-mediated repair. Furthermore, the work reported here and that presented in Miura *et al.* (2013) utilize significantly different plasmid repair assays. While the Miura *et al.* (2013) assay limits repair events exclusively to SDSA, the plasmid-based assay used here allows either NCO or CO pathways. The significant differences in these assays may be the underlying cause for the observed SDSA effects.

Lastly, while *srs2-F891A* exhibited a clear shift from NCO to CO repair products in the plasmid-based gap repair system, this shift is not observed in the ectopic physical recombination assay. A fundamental difference between the two assays is the extent to which the broken DNA substrates may be resected. In fact, a previous publication has shown that, unlike chromosome-based recombination assays, loss of DNA resection enzymes actually improves overall repair efficiency in the plasmid-based gap repair system (Guo and Jinks-Robertson 2013). This is largely attributed to destruction of linearized plasmids by Exo1- or Sgs1-Dna2-mediated long-range resection before repair can take place. We can thus infer that the transformants isolated from such plasmid-based gap repair assays correspond to a minority of repair events that have escaped extensive resection. Assuming this, the resulting D-loops may vary with respect to their size and overall stability. If Srs2 does, in fact, promote SDSA by dissolving extended D-loops, then the presumably longer and more stable D-loops in chromosome-based recombination assays may be refractory to Srs2-mediated dissolution.

Another difference between both crossover systems is homology length. The plasmid-based crossover system has ~400-bp homologies flanking the DSB (Mitchel *et al.* 2010, 2013); in the chromosomal system ~1400-bp and 500-bp homologies flank the DSB (Ira *et al.* 2003). It is possible that the shorter homology results in different types or sizes of D-loops that are more dependent on processing by Srs2. Unfortunately, physical chromosomal systems with homology lengths similar to the plasmid-based system do not result in measurable crossover frequencies (Inbar *et al.* 2000), making it difficult to test the homology length parameter.

Alternatively, as it has been proposed by Prado and Aguilera (2003), extensively resected DNA substrates with limited homology to the donor sequence are likely channeled into the SDSA subpathway, producing exclusively NCO repair products (Prado and Aguilera 2003). Therefore, extensive resection of chromosomal substrates, such as the chromosomal substrates in the ectopic physical assay used here, likely commits the intermediates to the SDSA subpathway. The extensively resected chromosomes can persist until repaired through SDSA, consequently minimizing the effect Srs2 may have on the CO to NCO ratios. In contrast, the broken ends in the plasmid-based gap repair system may have a very short and transient window to successfully repair the gap, beyond which they become degraded and unrepairable. The minimally resected broken ends maintain the capacity to go through the dHJ pathway with the potential to still generate CO repair products as well as NCOs. Therefore, Srs2 activity on such substrates can still measurably sway the relative frequency of repair products.

In summary, we have identified a novel *srs2* mutation that, at least in part, behaves as a separation-of-function mutation that specifically inactivates the Srs2 pro-SDSA function in the plasmid-based gap repair system while maintaining its anti-recombination function. Our findings reveal the complexity of the Srs2–Rad51 interaction and suggest a possible role for the Srs2–Rad51 interaction in SDSA/CO regulation.

Acknowledgments

We are grateful to James Haber, Giordano Liberi, and Roger Brent for providing us with yeast strains, and Akira Shinohara for providing us with the anti-Rad51 rabbit serum. This work was supported by the National Institutes of Health (S.C.K.: GM64745, S.-J.R.: GM38464, W.-D.H.: GM58015, CA92276). This research used core services supported by P30 CA93373. The funders had no role in study design, data collection and analysis, decision to publish, or preparation of the manuscript.

Literature Cited

Aboussekhra, A., R. Chanet, Z. Zgaga, C. Cassier Chauvat, M. Heude *et al.*, 1989 *RADH*, a gene of *Saccharomyces cerevisiae* encoding a putative DNA helicase involved in DNA repair. Characteristics of *radH* mutants and sequence of the gene. Nucleic Acids Res. 17: 7211–7219. https://doi.org/10.1093/nar/17.18.7211

Aboussekhra, A., R. Chanet, A. Adjiri, and F. Fabre, 1992 Semidominant suppressors of Srs2 helicase mutations of *Saccharomyces cerevisiae* map in the *RAD51* gene, whose sequence predicts a protein with similarities to procaryotic RecA protein. Mol. Cell. Biol. 12: 3224–3234. https://doi.org/10.1128/MCB.12.7.3224

Aguilera, A., and H. L. Klein, 1988 Genetic control of intrachromosomal recombination in *Saccharomyces cerevisiae*. I. Isolation and genetic characterization of hyper-recombination mutations. Genetics 119: 779–790.

Antony, E., E. J. Tomko, Q. Xiao, L. Krejci, T. M. Lohman *et al.*, 2009 Srs2 disassembles Rad51 filaments by a protein-protein interaction triggering ATP turnover and dissociation of Rad51 from DNA. Mol. Cell 35: 105–115. https://doi.org/10.1016/j.molcel.2009.05.026

Armstrong, A. A., F. Mohideen, and C. D. Lima, 2012 Recognition of SUMO-modified PCNA requires tandem receptor motifs in Srs2. Nature 483: 59–63. https://doi.org/10.1038/nature10883

Aylon, Y., B. Liefshitz, G. Bitan-Banin, and M. Kupiec, 2003 Molecular dissection of mitotic recombination in the yeast *Saccharomyces cerevisiae*. Mol. Biol. Cell 23: 1403–1417. https://doi.org/10.1128/MCB.23.4.1403-1417.2003

Bashkirov, V. I., J. S. King, E. V. Bashkirova, J. Schmuckli-Maurer, and W. D. Heyer, 2000 DNA repair protein Rad55 is a terminal substrate of the DNA damage checkpoints. Mol. Cell. Biol. 20: 4393–4404. https://doi.org/10.1128/MCB.20.12.4393-4404.2000

Bienko, M., C. M. Green, N. Crosetto, F. Rudolf, G. Zapart *et al.*, 2005 Ubiquitin-binding domains in Y-family polymerases regulate translesion synthesis. Science 310: 1821–1824. https://doi.org/10.1126/science.1120615

Bronstein, A., L. Gershon, G. Grinberg, E. Alonso-Perez, and M. Kupiec, 2018 The main role of Srs2 in DNA repair depends on its helicase activity, rather than on its interactions with PCNA or Rad51. MBio 9: e01192-18. https://doi.org/10.1128/mBio.01192-18

Burkovics, P., M. Sebesta, A. Sisakova, N. Plault, V. Szukacsov *et al.*, 2013 Srs2 mediates PCNA-SUMO-dependent inhibition of DNA repair synthesis. EMBO J. 32: 742–755. https://doi.org/10.1038/emboj.2013.9

Chanet, R., M. Heude, A. Adjiri, L. Maloisel, and F. Fabre, 1996 Semidominant mutations in the yeast Rad51 protein and their relationships with the Srs2 helicase. Mol. Cell. Biol. 16: 4782–4789. https://doi.org/10.1128/MCB.16.9.4782

Chen, Y. H., K. Choi, B. Szakal, J. Arenz, X. Y. Duan *et al.*, 2009 Interplay between the Smc5/6 complex and the Mph1 helicase in recombinational repair. Proc. Natl. Acad. Sci. USA 106: 21252–21257. https://doi.org/10.1073/pnas.0908258106

Colavito, S., M. Macris-Kiss, C. Seong, O. Gleeson, E. C. Greene *et al.*, 2009 Functional significance of the Rad51-Srs2 complex in Rad51 presynaptic filament disruption. Nucleic Acids Res. 37: 6754–6764. https://doi.org/10.1093/nar/gkp748

Dupaigne, P., C. Le Breton, F. Fabre, S. Gangloff, E. Le Cam *et al.*, 2008 The Srs2 helicase activity is stimulated by Rad51 filaments on dsDNA: implications for crossover incidence during mitotic recombination. Mol. Cell 29: 243–254. https://doi.org/10.1016/j.molcel.2007.11.033

Fabre, F., A. Chan, W. D. Heyer, and S. Gangloff, 2002 Alternate pathways involving Sgs1/Top3, Mus81/Mms4, and Srs2 prevent formation of toxic recombination intermediates from single-stranded gaps created by DNA replication. Proc. Natl. Acad. Sci. USA 99: 16887–16892 [corrigenda: Proc. Natl. Acad. Sci. USA 100: 1462 (2003)]. https://doi.org/10.1073/pnas.252652399

Gangloff, S., C. Soustelle, and F. Fabre, 2000 Homologous recombination is responsible for cell death in the absence of the Sgs1 and Srs2 helicases. Nat. Genet. 25: 192–194. https://doi.org/10.1038/76055

Guo, X. G., and S. Jinks-Robertson, 2013 Roles of exonucleases and translesion synthesis DNA polymerases during mitotic gap repair in yeast. DNA Repair (Amst.) 12: 1024–1030. https://doi.org/10.1016/j.dnarep.2013.10.001

Harshman, K. D., W. S. Moye-Rowley, and C. S. Parker, 1988 Transcriptional activation by the SV40 AP-1 recognition element in yeast is mediated by a factor similar to AP-1 that is distinct from GCN4. Cell 53: 321–330. https://doi.org/10.1016/0092-8674(88)90393-5

Heyer, W. D., K. T. Ehmsen, and J. Liu, 2010 Regulation of homologous recombination in eukaryotes. Annu. Rev. Genet. 44: 113–139. https://doi.org/10.1146/annurev-genet-051710-150955

Hoege, C., B. Pfander, G. L. Moldovan, G. Pyrowolakis, and S. Jentsch, 2002 RAD6-dependent DNA repair is linked to modification of PCNA by ubiquitin and SUMO. Nature 419: 135–141. https://doi.org/10.1038/nature00991

Inbar, O., B. Liefshitz, G. Bitan, and M. Kupiec, 2000 The relationship between homology length and crossing over during the repair of a broken chromosome. J. Biol. Chem. 275: 30833–30838. https://doi.org/10.1074/jbc.C000133200

Ira, G., A. Malkova, G. Liberi, M. Foiani, and J. E. Haber, 2003 Srs2 and Sgs1-Top3 suppress crossovers during double-strand break repair in yeast. Cell 115: 401–411. https://doi.org/10.1016/S0092-8674(03)00886-9

Islam, M. N., N. Paquet, D. Fox, E. Dray, X. F. Zheng *et al.*, 2012 A variant of the breast cancer type 2 susceptibility protein (BRC) repeat is essential for the RECQL5 helicase to interact with RAD51 recombinase for genome stabilization. J. Biol. Chem. 287: 23808–23818. https://doi.org/10.1074/jbc.M112.375014

Jenkins, S. S., S. Mukherjee, and W.-D. Heyer, 2016 DNA repair by homologous recombination, pp. 456–467 in *Encyclopedia of Cell Biology*, edited by R. A. Bradshaw, and P. D. Stahl. Academic Press, Waltham, MA.

Kaniecki, K., L. De Tullio, B. Gibb, Y. Kwon, P. Sung *et al.*, 2017 Dissociation of Rad51 presynaptic complexes and heteroduplex DNA joints by tandem assemblies of Srs2. Cell Rep. 21: 3166–3177. https://doi.org/10.1016/j.celrep.2017.11.047

Keyamura, K., K. Arai, and T. Hishida, 2016 Srs2 and Mus81-Mms4 prevent accumulation of toxic inter-homolog recombination intermediates. PLoS Genet. 12: e1006136. https://doi.org/10.1371/journal.pgen.1006136

Kowalczykowski, S. C., N. Hunter, and W.-D. Heyer (Editors), 2016 *DNA Recombination*. Cold Spring Harbor Laboratory Press, Cold Spring Harbor, NY.

Krejci, L., S. Van Komen, Y. Li, J. Villemain, M. S. Reddy *et al.*, 2003 DNA helicase Srs2 disrupts the Rad51 presynaptic filament. Nature 423: 305–309. https://doi.org/10.1038/nature01577

Lawrence, C. W., and R. B. Christensen, 1979 Metabolic suppressors of trimethoprim and ultraviolet light sensitivities of *Saccharomyces cerevisiae rad6* mutants. J. Bacteriol. 139: 866–876.

Liu, J., C. Ede, W. D. Wright, S. K. Gore, S. S. Jenkins *et al.*, 2017 Srs2 promotes synthesis-dependent strand annealing by disrupting DNA polymerase delta-extending D-loops. eLife 6: e22195. https://doi.org/10.7554/eLife.22195

Liu, J., N. Qian, and S. W. Morrical, 2006 Dynamics of bacteriophage T4 presynaptic filament assembly from extrinsic fluorescence measurements of Gp32-single-stranded DNA interactions. J. Biol. Chem. 281: 26308–26319. https://doi.org/10.1074/jbc.M604349200

Liu, J., L. Renault, X. Veaute, F. Fabre, H. Stahlberg *et al.*, 2011 Rad51 paralogues Rad55-Rad57 balance the antirecombinase Srs2 in Rad51 filament formation. Nature 479: 245–248. https://doi.org/10.1038/nature10522

Lovett, S. T., and R. K. Mortimer, 1987 Characterization of null mutants of the *RAD55* gene of *Saccharomyces cerevisiae*: effects of temperature, osmotic strength and mating type. Genetics 116: 547–553.

Ma, E., P. Dupaigne, L. Maloisel, R. Guerois, E. Le Cam *et al.*, 2018 Rad52-Rad51 association is essential to protect Rad51 filaments against Srs2, but facultative for filament formation. eLife 7: e32744. https://doi.org/10.7554/eLife.32744

McVey, M., V. Y. Khodaverdian, P. Cerqueira, and W.-D. Heyer, 2016 Eukaryotic DNA polymerases in homologous recombination. Annu. Rev. Genet. 50: 393–421. https://doi.org/10.1146/annurev-genet-120215-035243

Mitchel, K., H. S. Zhang, C. Welz-Voegele, and S. Jinks-Robertson, 2010 Molecular structures of crossover and noncrossover intermediates during gap repair in yeast: implications for recombination. Mol. Cell 38: 211–222. https://doi.org/10.1016/j.molcel.2010.02.028

Mitchel, K., K. Lehner, and S. Jinks-Robertson, 2013 Heteroduplex DNA position defines the roles of the Sgs1, Srs2, and Mph1 helicases in promoting distinct recombination outcomes. PLoS Genet. 9: e1003340. https://doi.org/10.1371/journal.pgen.1003340

Miura, T., T. Shibata, and K. Kusano, 2013 Putative antirecombinase Srs2 DNA helicase promotes noncrossover homologous recombination avoiding loss of heterozygosity. Proc. Natl. Acad. Sci. USA 110: 16067–16072. https://doi.org/10.1073/pnas.1303111110

Niu, H. Y., and H. L. Klein, 2017 Multifunctional roles of *Saccharomyces cerevisiae* Srs2 protein in replication, recombination and repair. FEMS Yeast Res. 17: fow111. https://doi.org/10.1093/femsyr/fow111

Paliwal, S., R. Kanagaraj, A. Sturzenegger, K. Burdova, and P. Janscak, 2014 Human RECQ5 helicase promotes repair of DNA double-strand breaks by synthesis-dependent strand annealing. Nucleic Acids Res. 42: 2380–2390. https://doi.org/10.1093/nar/gkt1263

Palladino, F., and H. L. Klein, 1992 Analysis of mitotic and meiotic defects in *Saccharomyces cerevisiae SRS2* DNA helicase mutants. Genetics 132: 23–37.

Panico, E. R., C. Ede, M. Schildmann, K. A. Schurer, and W. Kramer, 2010 Genetic evidence for a role of *Saccharomyces cerevisiae* Mph1 in recombinational DNA repair under replicative stress. Yeast 27: 11–27. https://doi.org/10.1002/yea.1727

Pellegrini, L., D. S. Yu, T. Lo, S. Anand, M. Lee *et al.*, 2002 Insights into DNA recombination from the structure of a RAD51-BRCA2 complex. Nature 420: 287–293. https://doi.org/10.1038/nature01230

Piazza, A., S. S. Shah, W. D. Wright, S. K. Gore, R. Koszul *et al.*, 2019 Dynamic processing of displacement loops during recombinational DNA repair. Mol. Cell 73: 1255–1266.e4. https://doi.org/10.1016/j.molcel.2019.01.005

Prado, F., and A. Aguilera, 2003 Control of cross-over by single-strand DNA resection. Trends Genet. 19: 428–431. https://doi.org/10.1016/S0168-9525(03)00173-2

Prakash, R., D. Satory, E. Dray, A. Papusha, J. Scheller *et al.*, 2009 Yeast Mph1 helicase dissociates Rad51-made D-loops: implications for crossover control in mitotic recombination. Genes Dev. 23: 67–79. https://doi.org/10.1101/gad.1737809

Robert, T., D. Dervins, F. Fabre, and S. Gangloff, 2006 Mrc1 and Srs2 are major actors in the regulation of spontaneous crossover. EMBO J. 25: 2837–2846. https://doi.org/10.1038/sj.emboj.7601158

Rong, L., and H. L. Klein, 1993 Purification and characterization of the SRS2 DNA helicase of the yeast *Saccharomyces cerevisiae*. J. Biol. Chem. 268: 1252–1259.

Rong, L., F. Palladino, A. Aguilera, and H. L. Klein, 1991 The hyper-gene conversion *hpr5–1* mutation of *Saccharomyces cerevisiae* is an allele of the *SRS2/RADH* gene. Genetics 127: 75–85.

Sasanuma, H., Y. Furihata, M. Shinohara, and A. Shinohara, 2013 Remodeling of the Rad51 DNA strand-exchange protein by the Srs2 helicase. Genetics 194: 859–872. https://doi.org/10.1534/genetics.113.150615

Schiestl, R. H., J. Zhu, and T. D. Petes, 1994 Effect of mutations in genes affecting homologous recombination on restriction enzyme-mediated and illegitimate recombination in *Saccharomyces cerevisiae*. Mol. Cell. Biol. 14: 4493–4500. https://doi.org/10.1128/MCB.14.7.4493

Seong, C., S. Colavito, Y. Kwon, P. Sung, and L. Krejci, 2009 Regulation of Rad51 recombinase presynaptic filament assembly *via* interactions with the Rad52 mediator and the Srs2 anti-recombinase. J. Biol. Chem. 284: 24363–24371. https://doi.org/10.1074/jbc.M109.032953

Spell, R. M., and S. Jinks-Robertson, 2003 Role of mismatch repair in the fidelity of RAD51- and RAD59-dependent recombination in *Saccharomyces cerevisiae*. Genetics 165: 1733–1744.

Spell, R. M., and S. Jinks-Robertson, 2004a Determination of mitotic recombination rates by fluctuation analysis in *Saccharomyces cerevisiae*. Methods Mol. Biol. 262: 3–12.

Spell, R. M., and S. Jinks-Robertson, 2004b Examination of the roles of Sgs1 and Srs2 helicases in the enforcement of recombination fidelity in *Saccharomyces cerevisiae*. Genetics 168: 1855–1865. https://doi.org/10.1534/genetics.104.032771

Sung, P., 1994 Catalysis of ATP-dependent homologous DNA pairing and strand exchange by yeast RAD51 protein. Science 265: 1241–1243. https://doi.org/10.1126/science.8066464

Symington, L. S., and J. Gautier, 2011 Double-strand break end resection and repair pathway choice. Annu. Rev. Genet. 45: 247–271. https://doi.org/10.1146/annurev-genet-110410-132435

Tong, A. H. Y., G. Lesage, G. D. Bader, H. M. Ding, H. Xu *et al.*, 2004 Global mapping of the yeast genetic interaction network. Science 303: 808–813. https://doi.org/10.1126/science.1091317

Veaute, X., J. Jeusset, C. Soustelle, S. C. Kowalczykowski, E. Le Cam *et al.*, 2003 The Srs2 helicase prevents recombination by disrupting Rad51 nucleoprotein filaments. Nature 423: 309–312. https://doi.org/10.1038/nature01585

Warren, M., A. Smith, N. Partridge, J. Masabanda, D. Griffin *et al.*, 2002 Structural analysis of the chicken BRCA2 gene facilitates identification of functional domains and disease causing mutations. Hum. Mol. Genet. 11: 841–851. https://doi.org/10.1093/hmg/11.7.841

Welz-Voegele, C., and S. Jinks-Robertson, 2008 Sequence divergence impedes crossover more than noncrossover events during mitotic gap repair in yeast. Genetics 179: 1251–1262. https://doi.org/10.1534/genetics.108.090233

Xue, X. Y., A. Papusha, K. Y. Choi, J. N. Bonner, S. Kumar *et al.*, 2016 Differential regulation of the anti-crossover and replication fork regression activities of Mph1 by Mte1. Genes Dev. 30: 687–699. https://doi.org/10.1101/gad.276139.115

Communicating editor: D. Bishop